The American Journal of Pathology, Vol. 185, No. 4, April 2015

The American Journal of
PATHOLOGY
ajp.amjpathol.org

VASCULAR BIOLOGY, ATHEROSCLEROSIS, AND ENDOTHELIUM BIOLOGY

Selective Cathepsin S Inhibition Attenuates Atherosclerosis in Apolipoprotein E–Deficient Mice with Chronic Renal Disease

Jose-Luiz Figueiredo,* Masanori Aikawa,* Chunyu Zheng,* Jacob Aaron,* Lilian Lax,* Peter Libby,* Jose Luiz de Lima Filho,† Sabine Gruener,‡ Jürgen Fingerle,‡ Wolfgang Haap,‡ Guido Hartmann,‡ and Elena Aikawa*

From The Center of Excellence in Vascular Biology, Department of Medicine, Brigham and Women's Hospital, Harvard Medical School, Boston, Massachusetts; the Laboratory of Immunopathology Keizo Asami,† Federal University of Pernambuco, Recife, Brazil; and Pharma Research and Early Development,‡ Hoffman La Roche, Basel, Switzerland*

Accepted for publication November 25, 2014.

Address correspondence to Elena Aikawa, M.D., Ph.D., Brigham and Women's Hospital, Harvard Medical School, 77 Ave. Louis Pasteur, NRB-741, Boston, MA 02115. E-mail: eaikawa@partners.org.

Chronic renal disease (CRD) accelerates the development of atherosclerosis. The potent protease cathepsin S cleaves elastin and generates bioactive elastin peptides, thus promoting vascular inflammation and calcification. We hypothesized that selective cathepsin S inhibition attenuates atherogenesis in hypercholesterolemic mice with CRD. CRD was induced by 5/6 nephrectomy in high-fat high-cholesterol fed apolipoprotein E–deficient mice. CRD mice received a diet admixed with 6.6 or 60 mg/kg of the potent and selective cathepsin S inhibitor RO5444101 or a control diet. CRD mice had significantly higher plasma levels of osteopontin, osteocalcin, and osteoprotegerin (204%, 148%, and 55%, respectively; $P < 0.05$), which were inhibited by RO5444101 (60%, 40%, and 36%, respectively; $P < 0.05$). Near-infrared fluorescence molecular imaging revealed a significant reduction in cathepsin activity in treated mice. RO5444101 decreased osteogenic activity. Histologic assessment in atherosclerotic plaque demonstrated that RO5444101 reduced immunoreactive cathepsin S ($P < 0.05$), elastin degradation ($P = 0.01$), plaque size ($P = 0.01$), macrophage accumulation ($P < 0.01$), growth differentiation factor-15 ($P = 0.0001$), and calcification (alkaline phosphatase activity, $P < 0.01$; osteocalcin, $P < 0.05$). Furthermore, cathepsin S inhibitor or siRNA significantly decreased expression of growth differentiation factor-15 and monocyte chemotactic protein-1 in a murine macrophage cell line and human primary macrophages. Systemic inhibition of cathepsin S attenuates the progression of atherosclerotic lesions in 5/6 nephrectomized mice, serving as a potential treatment for atherosclerosis in patients with CRD. *(Am J Pathol 2015, 185: 1156–1166; http://dx.doi.org/10.1016/j.ajpath.2014.11.026)*

Half of all patients with chronic renal disease (CRD) die of cardiovascular causes.[1,2] Patients with early stages of CRD who are not undergoing dialysis have cardiovascular disease (CVD) risk similar to that of patients with established coronary artery disease,[3] whereas patients with end-stage renal disease, treated by dialysis, have an approximately 30 times greater CVD risk than the general population.[4,5] Despite being at elevated risk for CVD, patients with CRD have experienced limited benefits from statin treatment alone.[6,7] Hence, the need is emerging to investigate the mechanisms responsible for CVD in CRD patients to develop effective new therapies.

Arterial inflammation is a key facet of atherosclerotic lesion initiation and progression.[8,9] Several molecular mechanisms participate in the response to injuries at the vascular wall and in the formation and progression of atherosclerotic lesions.[10] Chronic inflammation likely accelerates atherosclerosis in patients with CRD,[11] and the combination of chronic inflammation and an imbalance in the calcium phosphate serum level in these patients exacerbates these processes.[12,13] In addition, CRD patients receiving hemodialysis have elevated levels of

Supported by investigator-initiated research grant 2010A052417 from Hoffmann-La Roche Ltd. (E.A.) and by NIH grants R01HL114805 and R01HL109506 (E.A.), R01HL107550 (M.A.), and R01HL80472 (P.L.).

Disclosures: S.G., J.F., W.H., and G.H. are employees of Hoffmann-La Roche Ltd., which also funded parts of this research.

http://dx.doi.org/10.1016/j.ajpath.2014.11.026

circulating proinflammatory cytokines,[14] which can initiate and perpetuate the inflammation-calcification loop.

Cathepsin S plays a critical role in vascular inflammation and calcification. Monocyte-derived macrophages that mediate vascular inflammation express and secrete the cysteine protease cathepsin S.[15] At the basal membrane of the blood vessels, secreted cathepsin S cleaves several extracellular matrix proteins, including laminin, collagen, and, preferentially, elastin, which generate bioactive elastin peptides.[16,17] Elastin-derived peptides and fragments, also known as matrikines, can incite inflammation. Elastin peptides stimulate macrophage chemotaxis[18] and promote vascular inflammation and calcification.[19] In addition, cathepsin S co-localizes with regions of increased elastin breaks in atherosclerotic plaques.[20]

We previously reported that cathepsin S deficiency leads to reduced elastolytic activity and decreased vascular inflammation and calcification in the arteries of hypercholesterolemic mice with experimental CRD, providing *in vivo* evidence implicating cathepsin S–induced elastolysis in arterial and aortic valve calcification.[21] To seek a clinically translatable proof of concept, the present study tested the hypothesis that treatment with a highly selective cathepsin S inhibitor attenuates inflammation and atherosclerotic lesion formation in the arteries of hypercholesterolemic mice with CRD.

Materials and Methods

Animal Protocol

Male 10-week-old *Apoe*$^{-/-}$ mice ($N = 60$) from The Jackson Laboratory (Bar Harbor, ME) were fed a high-fat high-cholesterol diet (Teklad TD.88137; Harlan Laboratories, Indianapolis, IN) for 10 weeks. At 20 weeks of age, mice were randomized either to continue with the diet ($n = 15$) or to undergo 5/6 nephrectomy ($n = 45$). CRD mice were then treated with 6.6 or 60 mg/kg of RO5444101, a highly potent and selective cathepsin S inhibitor (Hoffmann-La Roche, Basel, Switzerland) ($n = 15$ per group), admixed with the high-fat high-cholesterol diet for an additional 10 weeks. The Harvard Medical School Standing Committee on Animals approved all the animal studies.

Cells and Reagents

Human peripheral blood mononuclear cells (PBMCs) were isolated by centrifugation in Ficoll-Hypaque (Sigma-Aldrich, St. Louis, MO) and adherence. Cells were cultured for 10 days in RPMI 1640 medium (Invitrogen, Carlsbad, CA) supplemented with 5% heat-inactivated human serum, 2 mmol/L L-glutamine, 100 μg/mL penicillin, and 100 U/mL streptomycin to differentiate into macrophages. Murine macrophage-like RAW264.7 cells were purchased from ATCC (Manassas, VA) and grown in Dulbecco's modified Eagle's medium with 10% fetal bovine serum.

Surgically Induced CRD

We used an established model to induce chronic renal failure by controlling the amount of kidney mass removed.[21] This procedure includes two steps to create uremia.[21,22] First, we performed 2/3 nephrectomy, removing the top one-third and bottom one-third of the left kidney. Then, after 7 days of healing, the right kidney was removed.

Molecular Imaging of Cathepsin Activity and Osteogenesis

Twenty-four hours before imaging, mice received simultaneous i.v. injections of two spectrally distinct molecular imaging agents: a protease-activatable, pan-cathepsin fluorescent agent (ProSense 750; PerkinElmer, Waltham, MA) and a bisphosphonate-conjugated calcium tracer (OsteoSense 680; PerkinElmer). Dual-channel (633 nm for excitation and 748 nm for emission) *in vivo* near-infrared fluorescence (NIRF) of carotid arteries was acquired using a laser scanning multicolor fluorescence microscope (Olympus Corp, Tokyo, Japan), as previously described elsewhere.[23,24] For *ex vivo* NIRF reflectance imaging, we perfused the heart with saline solution to flush out blood. Aortas and arteries were dissected and then were imaged using an NIRF reflectance imaging system (Image Station 4000MM; Eastman Kodak Co., New Haven, CT). Image stacks were processed and analyzed using ImageJ software version 1.41 (NIH, Bethesda, MD). Mice were then sacrificed for correlative histologic analyses of the aorta and arteries.

Quantification of Compound Plasma Levels and p10 Accumulation in Spleens

Male 8-week-old wild-type mice ($N = 8$; Charles River Laboratories, Sulzfeld, Germany) received RO5444101, and terminal blood samples were collected at seven different time points in precooled EDTA-coated tubes. The samples were kept on ice and immediately centrifuged at 4°C to obtain plasma. Quantification of compound levels in plasma was performed by liquid chromatography–tandem mass spectrometry analysis. Increased p10 was confirmed in spleens, which were homogenized in radioimmunoprecipitation assay buffer with protease inhibitors. Lysates were electrophoresed, and proteins were transferred to polyvinylidene difluoride membrane. Membrane was incubated with CD74 primary antibody (BD Pharmingen, Heidelberg, Germany) and then with anti-rabbit secondary antibody. The membrane was developed by Western blot analysis (GE Healthcare, Buckinghamshire, UK).

Quantification of Blood Proteins

Blood was collected via the inferior vena cava and was spun in a refrigerated centrifuge; serum was stored at −80°C. Serum levels of osteogenic markers, including

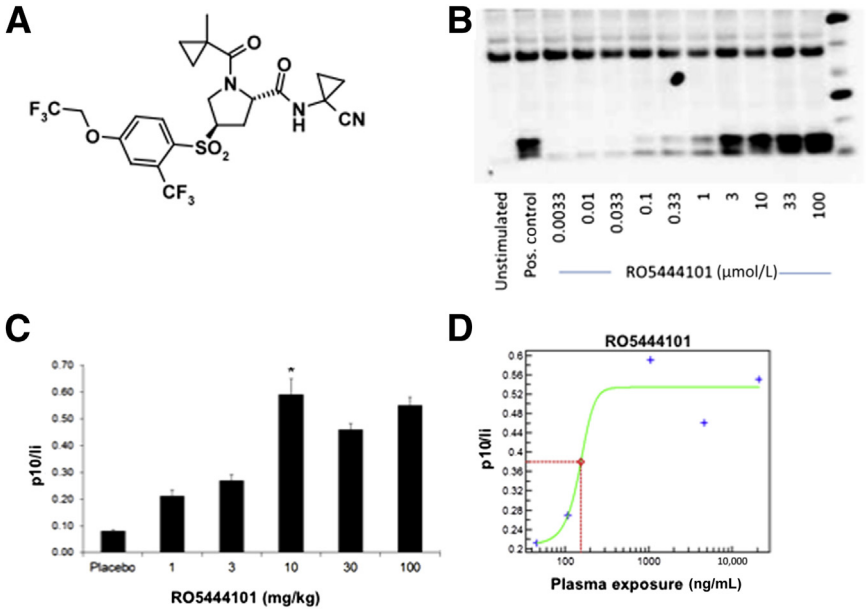

Figure 1 Pharmacology of RO5444101, a specific inhibitor of cathepsin S. **A:** The structure of the selective cathepsin S inhibitor RO5444101. **B:** Human B cells isolated from peripheral blood mononuclear cells were treated with increasing concentrations of RO5444101, followed by Western blot analysis to quantify accumulation of p10. **C:** Effects of cathepsin S compound on p10 accumulation *in vivo*. Significant p10 accumulation was observed at a 10-mg/kg dose. **D:** The plasma concentration of RO5444101 compound in relationship to p10 accumulation. The **green line** depicts the p10 elevation depending on drug plasma concentration (plasma exposure); **red line**, the half maximal concentration of drug in plasma to achieve p10 elevation (EC50); **blue plus signs**, measurements for the green curve. Data represent means ± SD. $*P < 0.05$.

bone gamma-carboxylglutamate (gla) protein or osteocalcin, secreted phosphoprotein 1 or osteopontin, and osteoprotegerin or tumor necrosis factor receptor superfamily, member 11b, were measured by sandwich enzyme-linked immunosorbent assay kits (Millipore, Billerica, MA).

Histopathologic Assessment

Tissue samples were frozen in optimum cutting temperature compound (Sakura Finetek, Torrence, CA), and 6-μm serial sections were cut and stained with hematoxylin and eosin for general morphologic evaluation. Alkaline phosphatase activity was detected on cryosections (alkaline phosphatase substrate kit; Vector Laboratories, Burlingame, CA). Van Gieson stain was used to assess elastin. Immunohistochemical analysis for macrophages (anti-mouse mac3; BD Biosciences, San Jose, CA), cathepsin S (anti-mouse cathepsin S; Santa Cruz Biotechnology, Santa Cruz, CA), osteocalcin (goat anti-mouse polyclonal antibody; Serotech, Dusseldorf, Germany), and growth differentiation factor-15 (GDF15) (rabbit anti−Gdf-15 polyclonal antibody; Bioss Antibodies, Woburn, MA) was performed using the avidin-biotin peroxidase method. Images were captured and processed using an Eclipse 80i microscope (Nikon Instruments, Melville, NY). Serial or adjacent sections were used for analyses of quantitative data. Double immunofluorescence staining was performed using cathepsin S antibodies and either mac3 or α-smooth muscle actin (clone 1A4; Sigma-Aldrich). Sections were counterstained with DAPI to visualize nuclei. Images were processed using an Eclipse confocal microscope system (Nikon Instruments).

siRNA Transfection

RAW264.7 cells were transfected with 200 nmol/L siRNA against cathepsin S or control scrambled nontargeting siRNA (Dharmacon, Lafayette, CO) using Lipofectamine 2000 (Invitrogen) for 48 hours before experiments, following the manufacturer's protocols. By this method, the silencing efficiency was consistently >90%.

Quantification of Gene Expression by Quantitative RT-PCR

Total RNA from human and murine macrophages was isolated using an RNeasy kit (Qiagen GmbH, Hilden, Germany) and was reverse transcribed by SuperScript II Reverse Transcriptase (Invitrogen) and oligo (dT) primers. Quantitative PCR was performed in the MyiQ single-color real-time PCR detection system (Bio-Rad Laboratories, Hercules, CA). The following primers from Integrated DNA Technologies (Coralville, IA) were used: hGDF-15: forward 5′-GACCCTCAGAGTTG-

Table 1 Species and Protease Selectivity of the Cathepsin S Inhibitor RO5444101

	50% Inhibitory concentration (nmol/L)					
RO compound	Human CatS	Mouse CatS	Dog CatS	Rabbit CatS	Human CatV or L2	Human CatK, CatL, CatC, CatX, CatH
RO5444101	0.2	0.3	7.9	0.4	2849.0	All >25,000

In vitro effects of RO5444101 on recombinant cathepsin S from different species and various human proteinases. The compound showed high potency and selectivity over other cathepsins in humans. This compound also shows high potency against cathepsin S in animals.

Cat, cathepsin.

Table 2 EC_{50} Values of the Cathepsin S Inhibitor RO5444101

RO compound	EC_{50} (nmol/L)						
	D1	D2	D3	D4	D5	D6	Mean ± SD
RO5444101	328.5	174.9	178.9	170.9	164.3	118.0	189.3 ± 71.7

D, donor.

CACTCC-3′ and reverse 5′-GCCTGGTTAGCAGGTCCTC-3′; mGDF-15: forward 5′-AGCTGCTACTCCGCGTCAA-3′ and reverse 5′-GTAAGCGCAGTTCCAGCTG-3′; hMCP-1/CCL2: forward 5′-CAGCCAGATGCAATCAATGCC-3′ and reverse 5′-TGGAATCCTGAACCCACTTCT-3′; and mMCP-1/CCL2: forward 5′-AGGTCCCTGTCATGCTTCTG-3′ and reverse 5′-TCTGGACCCATTCCTTCTTG-3′. The mRNA levels of the various genes tested were normalized to glyceraldehyde-3-phosphate dehydrogenase levels for human samples and to β-actin levels for murine samples.

Experiments on the Pharmacology of Cathepsin S Inhibitor and p10 Assay

Enzymatic activity was measured by observing the increase in fluorescence intensity caused by cleavage of a peptide substrate containing a fluorophore, the emission of which is quenched in the intact peptide. The assay buffer consisted of 100 mmol/L potassium phosphate, pH 6.5, 5 mmol/L EDTA-Na, 0.001% Triton X-100 (Roche Diagnostics GmbH, Mannheim, Germany), and 5 mmol/L dithiothreitol. The enzymes (all at 1 nmol/L) used were as follows: human and mouse cathepsins S, K, L, and B were measured. Substrate (20 μmol/L): Z-Val-Val-Arg-AMC, except for cathepsin K, which uses Z-Leu-Arg-AMC (both from Bachem, Bubendorf, Sweden). Excitation was 360 nm, and emission was 465 nm. Enzyme was added to the substance dilutions in 96-well microtiter plates, and the reaction was started with substrate. Fluorescence emission was measured over 20 minutes.

Invariant chain p10 accumulation was detected in human B cells by Western blot analysis. B cells were purified from human PBMCs, with further purification of B cells using a $CD19^+$ affinity bead purification kit (Miltenyi Biotec GmbH, Bergisch Gladbach, Germany). Cells were stimulated with indicated concentrations of RO5444101 for 16 hours and then were homogenized in radioimmunoprecipitation assay buffer with protease inhibitors. Lysates were electrophoresed, and proteins were transferred to polyvinylidene difluoride membrane. Membrane was incubated with CD74 primary antibody Pin.1 and goat anti-mouse IgG—horseradish peroxidase (Art. 32430; Pierce Biotechnology, Rockford, IL). The membrane was developed by Western blot analysis (GE Healthcare).

Statistical Analysis

Data are presented as means ± SEM. Analysis of variance and Student's *t*-test were performed using GraphPad Prism software version 5.0 (GraphPad Software Inc., San Diego, CA).

Results

Structure and Pharmacology of a Specific Cathepsin S Inhibitor

This study used RO5444101, an inhibitor with high specificity to cathepsin S but not other cathepsins (Figure 1A). This compound inhibits the active site of cathepsin S with high potency (inhibitory constant was 0.13 nmol/L using an *in vitro* peptide cleavage assay) and good selectivity over other cathepsins (B, K, L, C, H, V, and X) or noncysteine proteases, tested to concentrations of up to 10 μmol/L (Table 1). The cellular activity of the compound was tested in assays of antigen presentation in human B cells. Cathepsin S cleaves critically the invariant chain, a chaperone of the major histocompatibility complex class II molecule. Inhibition of cathepsin S in antigen-presenting cells results in the accumulation of an intermediate of the invariant chain—p10—as determined by Western blot analysis (Figure 1B). The mean EC_{50} of RO5444101 was determined to be 189.3 nmol/L (Table 2). We also tested the effects of this compound in mice and observed that it significantly induced p10 accumulation in spleen extracts, demonstrating its *in vivo* efficacy (Figure 1, C and D). Reduced invariant cleavage, in turn, reduces surface major histocompatibility complex class II levels and the antigen-induced cytokine response in PBMCs. Inhibition of cathepsin S is, therefore, of great interest in

Table 3 Treatment with Cathepsin S Inhibitor Decreases Plasma Levels of Osteocalcin, Osteopontin, and Osteoprotegerin in *Apoe*$^{-/-}$ Mice with CRD Compared with Those without Treatment

Mouse group	Osteocalcin (ng/mL)	Osteopontin (ng/mL)	Osteoprotegerin (ng/mL)
Apoe$^{-/-}$	64.6 ± 28.1	1079.4 ± 300.1	1.8 ± 0.5
Apoe$^{-/-}$ CRD	161.3 ± 50.5*†	3275.1 ± 1181.0*†	2.8 ± 0.9*†
Apoe$^{-/-}$ CRD + 6.6 mg/kg	113.6 ± 61.6*	1832.7 ± 1109.0*	2.2 ± 0.7*
Apoe$^{-/-}$ CRD + 60 mg/kg	96.4 ± 20.1†	1294.3 ± 478.2†	1.8 ± 0.4†

Blood samples were collected from *Apoe*$^{-/-}$ mice at the end of the treatment period, and plasma levels of the osteogenic cytokines were measured by enzyme-linked immunosorbent assay.

*$P < 0.05$ between the low-dose treatment group (6.6 mg/kg) and the CRD group.

†$P < 0.05$ between the high-dose treatment group (60 mg/kg) and the CRD group.

CRD, chronic renal disease.

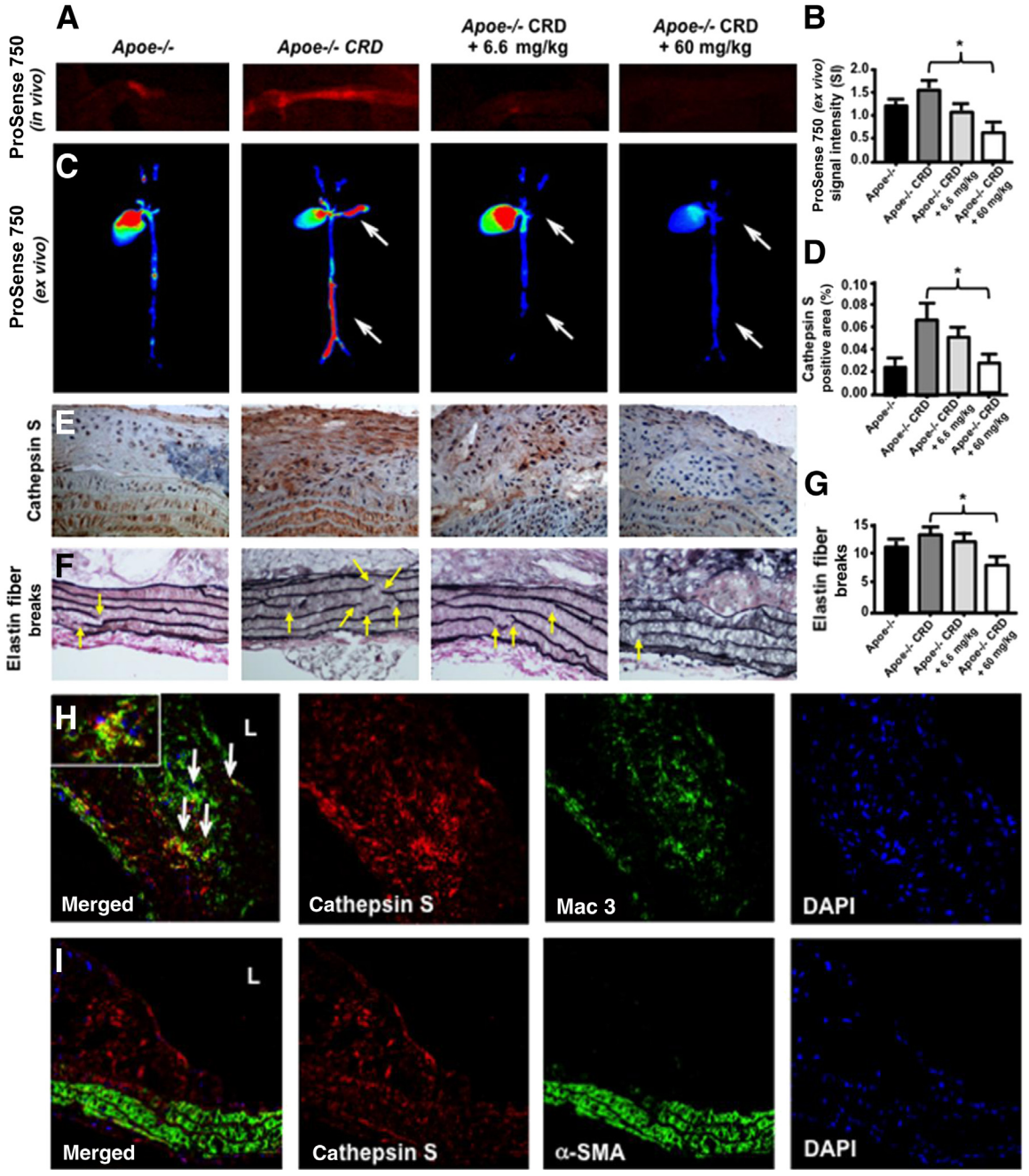

Figure 2 Effects of the cathepsin S inhibitor RO5444101 on cathepsin expression and activity in arteries of *Apoe*$^{-/-}$ mice with chronic renal disease (CRD). **A:** Representative microscopy images of cathepsin activity in the carotid arteries of live animals. **B** and **C:** Cathepsin activity in the entire aorta and carotid arteries using *ex vivo* fluorescence reflectance imaging. Note an increased cathepsin activity signal in the carotid arteries and abdominal aorta of *Apoe*$^{-/-}$ mice with CRD, which is diminished in the treated groups (**white arrows**). Quantification (**B**) and representative *ex vivo* near-infrared fluorescent reflectance images (**C**). **D** and **E:** Representative immunohistochemical staining images of cathepsin S in the aortic arch. **F** and **G:** Elastin fiber breaks (**yellow arrows**) detected by van Gieson staining (**F**) and quantified elastin fiber breaks (**G**) in the lesser curvature of the aortic arch. **H** and **I:** Cathepsin S co-localization with macrophages (**white arrows**) and smooth muscle cells in *Apoe*$^{-/-}$ mice with CRD. **H**, **inset**: Enlarged macrophage co-expressing cathepsin S. **L** indicates lumen. Data represent means ± SD. $^{*}P < 0.05$. Original magnification: ×400.

chronic inflammatory diseases because it may reduce tissue damage and dampen the generation of autoimmunity. Overall, RO5444101 compound shows good bioavailability and pharmacokinetic properties in mice and cynomolgus monkeys, making it an attractive small molecule inhibitor to study the function of cathepsin S in the context of chronic inflammatory diseases, including atherosclerosis.

Treatment with a Specific Cathepsin S Inhibitor Attenuates the Increase in Plasma Levels of Osteogenic Markers in *Apoe*$^{-/-}$ Mice with CRD

Plasma levels of osteocalcin [or bone gamma-carboxyglutamate (gla) protein], osteopontin (or secreted phosphoprotein 1), and osteoprotegerin (or tumor necrosis factor receptor superfamily,

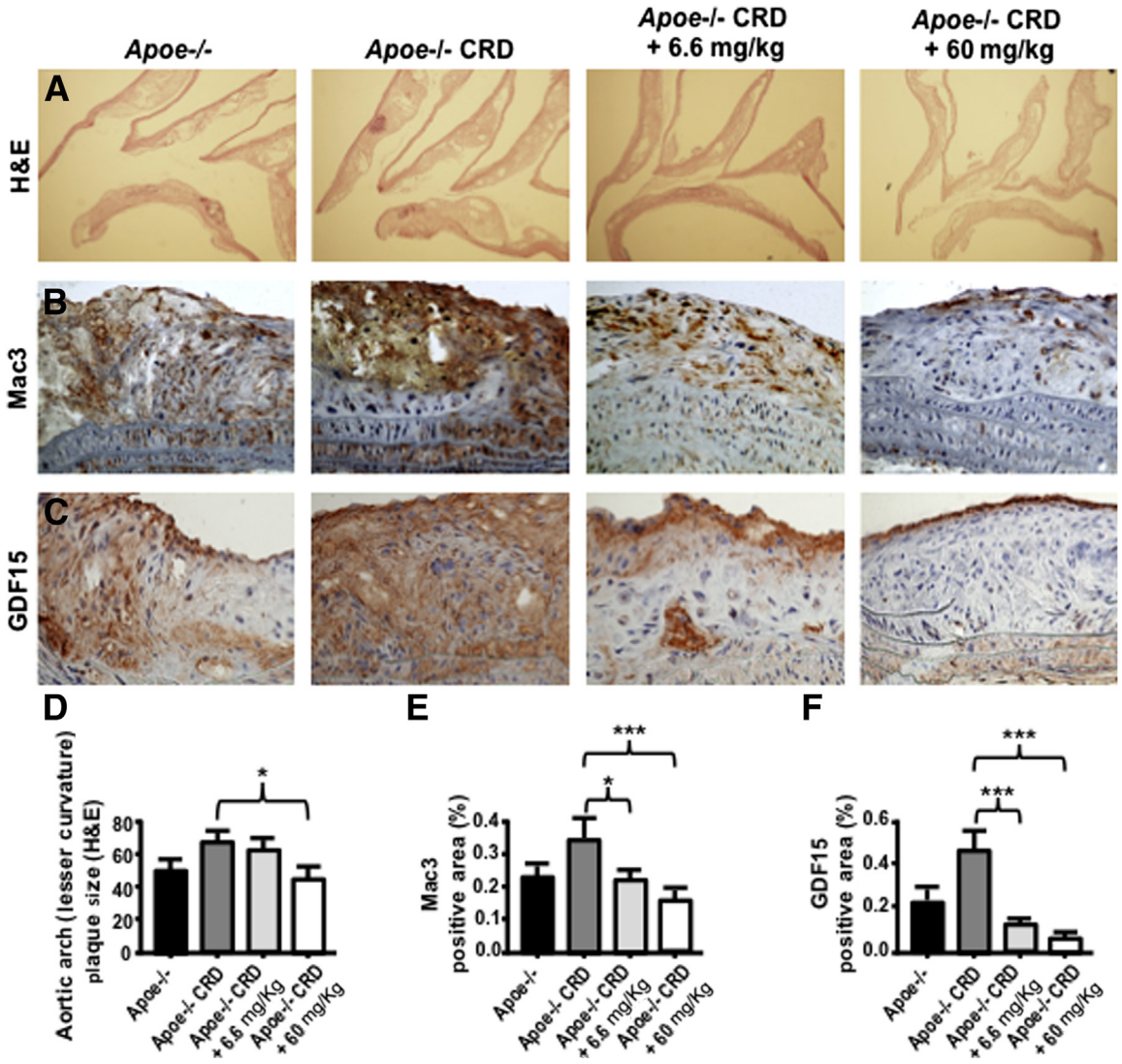

Figure 3 Cathepsin S inhibitor RO5444101 decreases plaque size, macrophage accumulation, and growth differentiation factor-15 (GDF15) expression in the atherosclerotic arteries of *Apoe*$^{-/-}$ mice with chronic renal disease (CRD). **A** and **D:** Quantification of atherosclerotic plaque size at the lesser curvature of the aortic arch using hematoxylin and eosin (H&E) staining. **B** and **E:** Mac3 staining in the aortic arch (**B**) shows macrophage accumulation on representative images; quantitative analysis of Mac3 staining (**E**). **C** and **F:** Immunohistochemical staining for a proinflammatory cytokine, GDF15, in the aortic arch (**C**) and its quantification (**F**). Data represent means ± SD. *$P < 0.05$, ***$P < 0.001$.

member 11b) increased in mice with CRD after 5/6 nephrectomy (Table 3). Treatment of CRD mice with the cathepsin S inhibitor RO5444101 attenuated these elevations. We observed dose-dependent decreases in plasma levels of osteocalcin ($P < 0.05$, 6 mg/kg; $P < 0.001$, 60 mg/kg), osteopontin ($P < 0.05$, 6 mg/kg; $P < 0.01$, 60 mg/kg), and osteoprotegerin ($P < 0.05$, 6 mg/kg; $P = 0.001$, 60 mg/kg) compared with CRD alone (Table 3). These results indicate that RO5444101 at 60 mg/kg reduced CRD-associated elevation of these proinflammatory and pro-osteogenic markers to normal levels.

RO5444101 Treatment Reduces Arterial Cathepsin Activity in CRD Mice

Intravital multichannel, high-resolution laser scanning fluorescence microscopy visualized *in vivo* real-time overall cathepsin activity with ProSense 750, a protease-activatable NIRF *in vivo* imaging agent that is activated by cathepsins, including cathepsins B, L, and S. Mice with CRD showed enhanced proteolytic signals in the carotid arteries compared with control animals, an effect that cathepsin S inhibitor treatment limited (Figure 2A). In addition, we used *ex vivo* macroscopic fluorescence reflectance imaging to map cathepsin activity in the aorta and carotid arteries. We observed a significant reduction in ProSense 750 signals in mice treated with RO5444101 ($P < 0.01$, 60 mg/kg dose versus CRD group) (Figure 2, B and C). Immunohistochemical analysis showed that cathepsin S inhibitor treatment attenuated CRD-induced accumulation of cathepsin S in the atherosclerotic plaques (Figure 2, D and E). Together, the molecular imaging and immunohistochemical analysis results suggested that cathepsin S inhibitor treatment reduced

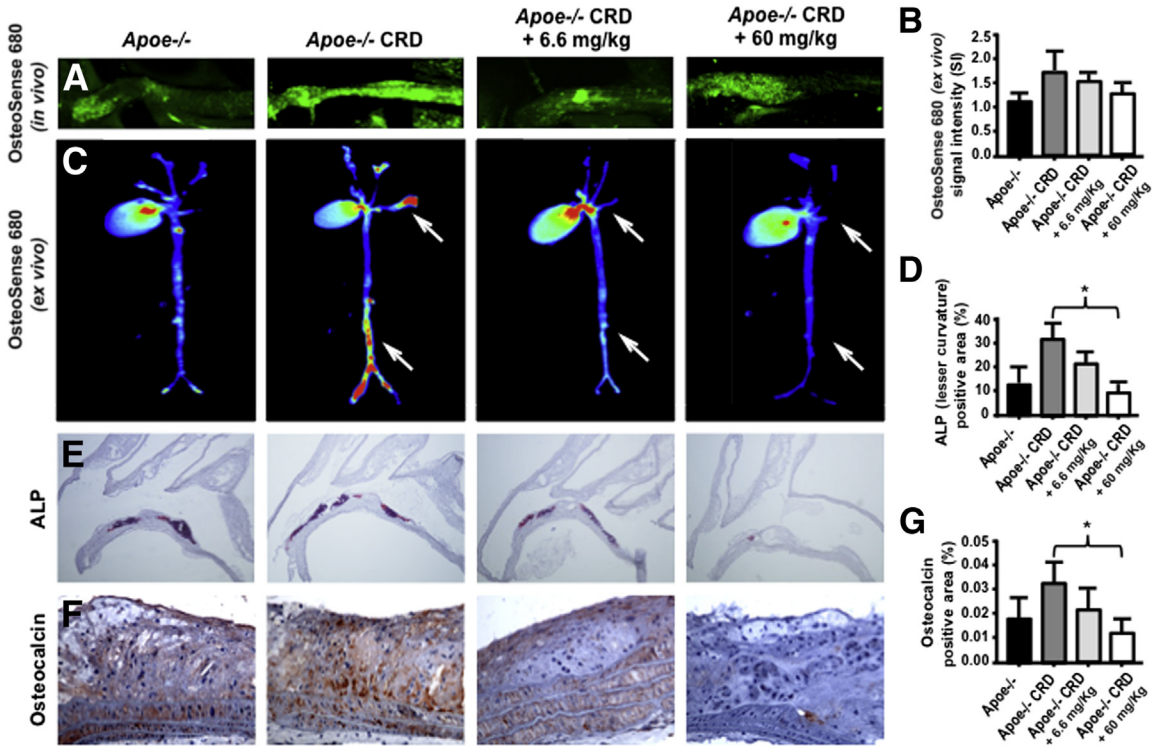

Figure 4 Cathepsin S inhibition decreases osteogenic activity in the atherosclerotic aorta and carotid arteries of *Apoe*$^{-/-}$ mice with chronic renal disease (CRD). **A:** Representative microscopic images of vascular calcification in the carotid arteries using a calcium-sensitive tracer (OsteoSense 680) in live animals. **B** and **C:** Osteogenic activity (OsteoSense 680) in the entire aorta and carotid arteries using *ex vivo* fluorescence reflectance imaging. Note an increased osteogenic activity signal in the carotid arteries and abdominal aorta of *Apoe*$^{-/-}$ mice with CRD, which is diminished in the treated groups (**arrows**). Quantification (**B**) and representative *ex vivo* near-infrared fluorescent reflectance images (**C**). **D** and **E:** The activity of alkaline phosphatase (ALP) in the aortic arch. **F** and **G:** Immunohistochemical staining for osteocalcin in the aortic arch (**F**) and its quantification (**G**). Data represent means ± SD. *$P < 0.05$.

elastolytic activity and cathepsin S protein levels in the aorta of CRD mice. Cathepsin S is the most potent elastolytic enzyme. We, therefore, examined elastin fragmentation in the lesser curvature of aortic arches. We observed that high-dose RO5444101 treatment (60 mg/kg) significantly reduced the number of elastin fiber breaks, as detected by van Gieson stain ($P = 0.01$) (Figure 2, F and G). These results suggested that mice treated with a high dose of cathepsin S inhibitor had reduced amounts of cathepsin S and limited elastin breaks, suggesting that the specific inhibition of cathepsin S reduces elastin fragmentation. Fluorescence immunohistochemical analysis for cathepsin S, mac3, and α-smooth muscle actin in plaques from CRD mice identified the cell types responsible for cathepsin S expression (Figure 2, H and I). We found that cathepsin S localized predominantly in macrophages but that some cathepsin S expression was also observed in inflamed medial smooth muscle cells.

Cathepsin S Inhibition Reduces the Development of Atherosclerotic Plaques and Expression of the Inflammatory Marker GDF15 in CRD Mice

Apoe$^{-/-}$ CRD mice treated with the cathepsin S inhibitor RO5444101 had decreased plaque burden in the lesser curvature of the aortic arch ($P = 0.01$) (Figure 3, A and D). The experiments were designed to allow the atherosclerotic lesions to develop in *Apoe*$^{-/-}$ mice on a high-fat high-cholesterol diet for 10 weeks before the induction of CRD and cathepsin S inhibition for another 10 weeks. To provide clinically relevant findings, we examined the effects of the cathepsin S–specific inhibitor RO5444101 on established atherosclerotic plaques but not on the initiation of atherosclerosis. We clearly observed significant reductions in the lesion size (Figure 3D) and macrophage accumulation (Figure 3E) in *Apoe*$^{-/-}$ CRD mice treated with a high dose of inhibitor. More importantly, the treatment reduced the atheroma burden of *Apoe*$^{-/-}$ CRD mice to levels similar to those of *Apoe*$^{-/-}$ with no CRD. These results suggest that this compound can substantially retard the development of advanced atherosclerosis in CRD. To explore the possible mechanisms of plaque size reduction, we examined macrophage accumulation and activation. RO5444101 treatment decreased CRD-induced macrophage accumulation and activation in intima and media as gauged by immunostaining for mac3 ($P < 0.01$ for 6.6 mg/kg, and $P < 0.001$ for 60 mg/kg) (Figure 3, B and E) and GDF15 (or macrophage inhibitory cytokine-1; $P < 0.0001$ for 6.6 and

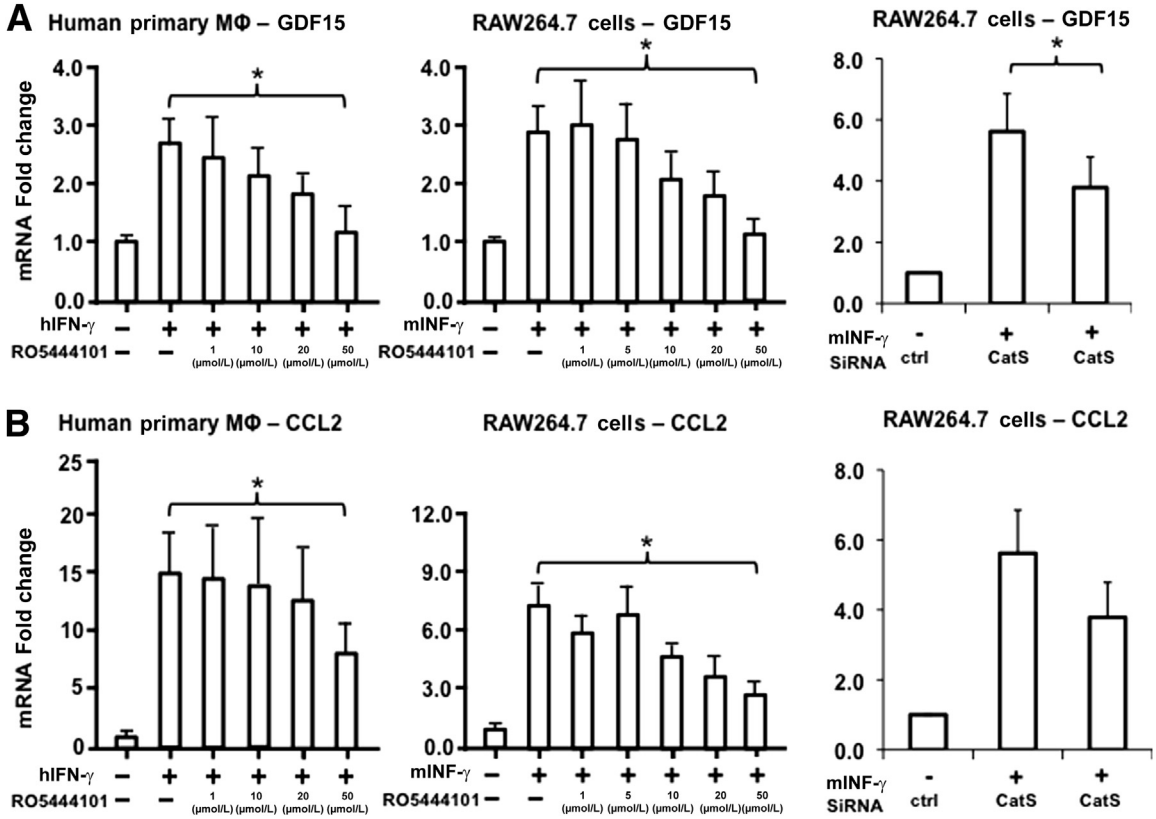

Figure 5 Cathepsin S (CatS)—specific inhibition by RO5444101 attenuates interferon γ (IFN-γ)—induced expression of growth differentiation factor-15 (GDF15) and monocyte chemotactic protein-1 (MCP-1)/CCL2 in human and mouse macrophages. Cultured human primary macrophages (MΦ) differentiated from peripheral blood monocytes and mouse macrophage-like RAW264.7 cells were pretreated with cathepsin S inhibitor RO5444101 and then were incubated with IFN-γ. RO5444101 or siRNA against cathepsin S reduced IFN-γ—induced GDF15 (**A**) and MCP-1/CCL2 (**B**) expression in both human and mouse macrophages. $N = 4$ for all experiments. Data represent means ± SD. $^*P < 0.05$ between comparisons. Ctrl, control; hIFN-γ, human IFN-γ; mIFN-γ, mouse IFN-γ.

60 mg/kg) (Figure 3, C and F). These results indicate that cathepsin S inhibition can reduce the inflammatory burden and halt and potentially even reverse atherosclerotic lesion formation in CRD. To demonstrate the cell source of cathepsin S expression, we performed double immunofluorescence labeling of cathepsin S and macrophages or smooth muscle cells. Staining showed that cathepsin S is predominantly expressed in medial and intimal macrophages (Figure 2H).

Cathepsin S Inhibition Reduces Arterial Calcification in CRD Mice

Apoe$^{-/-}$ CRD mice treated with 60 mg/kg of RO5444101 did not have significantly reduced osteogenic signals in the carotid arteries (*in vivo* NIRF imaging) (Figure 4A), aorta, and brachiocephalic arteries (*ex vivo* NIRF reflectance imaging) (Figure 4, B and C) as detected by the OsteoSense 680 calcium tracer. However, this treatment significantly lowered alkaline phosphatase activity ($P < 0.01$) (Figure 4, D and E) and osteocalcin expression ($P < 0.05$) (Figure 4, F and G) in the lesser curvature of aortic arches compared with the untreated group. Together, these results demonstrated that mice with CRD have enhanced osteogenic activities, which were reduced with cathepsin S inhibition.

RO5444101 Reduces IFN-γ—Induced GDF15 Expression in Human and Mouse Macrophages

The *in vivo* data suggested that cathepsin S—specific inhibition by RO5444101 reduced macrophage accumulation and expression of GDF15, a marker for macrophage activation, in the arteries of *Apoe*$^{-/-}$ CRD mice (Figure 3, B and C). The next question was whether a decrease in GDF15 resulted from reduced macrophages or whether this process also involved decreased macrophage activation. To test the hypothesis that cathepsin S inhibition reduces GDF15 expression by decreasing macrophage activation, we performed *in vitro* cell culture experiments. RO5444101 pretreatment reduced GDF15 expression induced by interferon γ (IFN-γ) in both human primary macrophages derived from peripheral blood monocytes (Figure 5A) and mouse macrophage-like RAW264.7 cells (Figure 5A). The RO5444101 effect seemed to involve cathepsin S inhibition, as siRNA silencing of the enzyme also reduced GDF15 induction by IFN-γ (Figure 5A). Similarly, RO5444101 or cathepsin S silencing by siRNA treatments

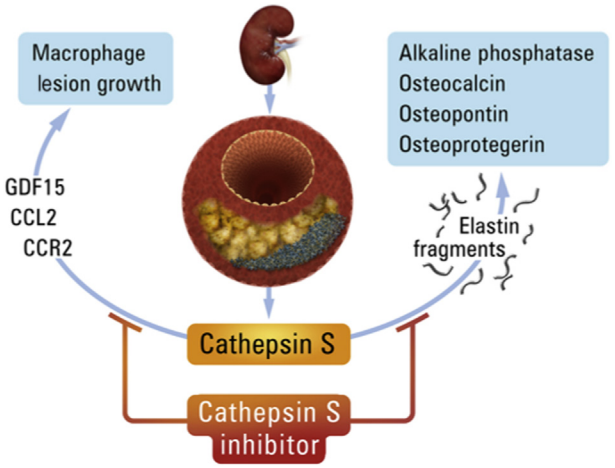

Figure 6 Cathepsin S inhibition in atherosclerotic plaques in chronic renal disease. Inhibition of cathepsin S may reduce lesion size via decreasing growth differentiation factor-15 (GDF15), a modulator of macrophage chemotaxis. Cathepsin S inhibition also may decrease osteogenic stimuli, such as osteopontin and osteocalcin, by suppressing elastin degradation. CCR2, C-C chemokine receptor type 2.

reduced IFN-γ–induced expression of monocyte chemotactic protein-1/CCL2, a proinflammatory chemokine (Figure 5B).

Discussion

More than half of all patients with CRD die of cardiovascular causes.[1,2] Despite their global health benefits, statins exert diminished effects in CRD patients.[5,6] We, therefore, need new therapies that alleviate cardiovascular risk in CRD patients. The present study provides evidence that specific and selective inhibition of cathepsin S reduces arterial inflammation and calcification in mice with CRD, suggesting a novel therapeutic target for reducing CVD risk in this patient population.

We observed that administration of the selective cathepsin S inhibitor RO5444101, which does not affect the proteolytic activity of other cathepsins, ameliorates several key features of arterial pathology in this animal model of accelerated atherosclerosis in CRD including i) reduction of atherosclerotic plaque size; ii) reduction of macrophage accumulation and activation in atherosclerotic plaques, as gauged by expression of mac3 and the proinflammatory molecule GDF15; iii) reduction of cathepsin activity and the number of elastin fiber breaks in the atherosclerotic plaques; iv) reduction of osteogenic activity and some features of vascular calcification; and v) reduction of plasma levels of circulating osteogenic markers. The results of RO5444101 action are summarized in Figure 6. These results show that elastolysis due to cathepsin S activity promotes vascular inflammation and calcification, supporting previous data in cathepsin S–deficient mice.[21] In addition, the present study results suggest that maintenance of elastin integrity by selective inhibition of cathepsin S activity reduces arterial inflammation and osteogenesis and may improve cardiovascular health in patients with CRD.

Cathepsin cysteine proteases such as cathepsin S play key roles in several CVDs, including aneurysm formation,[25] atherosclerosis,[26] and vascular calcification.[21] Cathepsin S is one of the most potent cysteine proteases, abundantly expressed by macrophages in atheroma. In the basal membrane of the blood vessel wall, cathepsin S acts as a potent elastolytic and collagenolytic protease, promoting arterial inflammation and atherosclerosis,[21,26] thus making it a promising target for therapeutic intervention.

We previously reported that genetically modified *Apoe*$^{-/-}$ mice lacking cathepsin S with surgically induced CRD showed significantly reduced elastin fragmentation and calcification in the arteries and aortic valves.[21] In this compound mutant strain, the expression of other cathepsins or matrix metalloproteinases did not change. We thus proposed that cathepsin S accelerates cardiovascular calcification via an elastolysis-dependent mechanism. The present study has extended previous work into a more translational investigation. Consistent with findings on cathepsin S–deficient mice, selective cathepsin S inhibition by administration of novel RO5444101 compound reduced elastin fragmentation in hypercholesterolemic *Apoe*$^{-/-}$ mice with CRD. Similarly, RO5444101 also reduced osteogenic activity in atherosclerotic arteries. Therefore, suppression of cathepsin S activity through either genetic or small molecule intervention yields similar results, lending additional support to a role for cathepsin S inhibition in the preservation of elastin integrity and vascular calcification.

The present study also examined the role of cathepsin S in atherosclerosis in mice with CRD and found that selective cathepsin S inhibition significantly reduces atherosclerotic plaque size. This effect likely resulted from reduced arterial inflammation, as we observed decreased plaque accumulation of macrophages. Macrophages promote the initiation and progression of atherosclerotic lesions, microcalcifications, plaque rupture, and acute thrombotic complications.[23,27] We reported previously that fragmentation of elastin fibers promotes inflammation.[21] Elastin-derived peptides/fragments exert proinflammatory effects, including macrophage chemoattraction[18] relevant to vascular pathophysiology.[19] Sukhova et al[26] reported that cathepsin S genetic deletion reduced atherosclerotic plaque size, macrophage accumulation, and proinflammatory cytokines in hypercholesterolemic low-density lipoprotein receptor–deficient mice. The present study observed similar findings in hypercholesterolemic apolipoprotein E–deficient mice with CRD suggesting that the presence of CRD, while accelerating atherosclerosis and inducing arterial calcification, did not negate the atheroprotective effects of cathepsin S inhibition.

GDF15/macrophage inhibitory cytokine-1 is a member of the transforming growth factor β superfamily and recently was recognized as a novel biomarker associated with CVD in the general population[28] and in patients with CRD.[29] Herein, we localized GDF15 protein in mac3-positive macrophages, and cathepsin S inhibition significantly reduced GDF15 accumulation in aortic lesions. Validation studies *in vitro* using primary macrophages and immortalized macrophage cell lines demonstrated that either cathepsin S inhibitor or siRNA reduced IFN-γ–induced macrophage GDF15 expression, consistent with the *in vivo* data. Therefore, GDF15, a known inducer of macrophage activation,[30] may contribute to the proinflammatory role of cathepsin S. Because GDF15 also independently predicts mortality risk in patients with CRD,[29] it may link atherosclerotic lesion development and CRD. GDF15 modulates macrophage chemotaxis in a strict C-C chemokine receptor type 2 and transforming growth factor β receptor type II–dependent manner.[31] We thus examined the effects of cathepsin S inhibition on CCL2—a C-C chemokine receptor type 2 ligand—and found that cathepsin S inhibition reduces macrophage expression of CCL2. Therefore, selective cathepsin S inhibition may inhibit macrophage recruitment in atherosclerotic lesions and reduce vascular inflammation and plaque development.

Complex positive feedback loops involving multifunctional regulators, such as cathepsin S, typically accelerate inflammation. It is, therefore, difficult to distinguish the direct effects of cathepsin S inhibition from secondary consequences *in vivo*. In addition to effects on macrophages and GDF15, this inhibitor reduces the surface major histocompatibility complex class II levels and the antigen-induced cytokine response in PBMCs. Moreover, gene deletion and pharmacological inhibition experiments in rodents demonstrate that cathepsin S participates in other cell types or contexts, such as reduced immune response of $CD4^+$ T cells and lower mobility of dendritic cells and B cells.[32,33] These mechanisms support cathepsin S as an attractive therapeutic target for immune diseases other than atherosclerosis, such as multiple sclerosis and rheumatoid arthritis.

In conclusion, the significantly elevated risk of cardiovascular morbidity and mortality in patients with CRD persisting after statin treatment calls for new therapeutic targets for intervention. Herein, we extend a previous mouse genetics study that demonstrated the impact of cathepsin S on cardiovascular inflammation and calcification by providing clinically translatable evidence. These findings support selective cathepsin S inhibition as a novel solution that may halt the progression of inflamed atherosclerotic lesions and prevent devastating cardiovascular complications in patients with CRD. Ongoing efforts that combine delineation of underlying molecular mechanisms and rigorous assessment of the cathepsin S inhibitor in patients will provide new insight into the optimal management of CVD in CRD patients.

Acknowledgments

We thank Whitney Irving, Eugenia Shvatrz, and Ling Ling Lok for technical assistance.

References

1. Campean V, Neureiter D, Varga I, Runk F, Reiman A, Garlichs C, Achenbach S, Nonnast-Daniel B, Amann K: Atherosclerosis and vascular calcification in chronic renal failure. Kidney Blood Press Res 2005, 28:280–289
2. Schiffrin EL, Lipman ML, Mann JF: Chronic kidney disease: effects on the cardiovascular system. Circulation 2007, 116:85–97
3. Foley RN, Parfrey PS, Sarnak MJ: Clinical epidemiology of cardiovascular disease in chronic renal disease. Am J Kidney Dis 1998, 32: S112–S119
4. de Jager DJ, Grootendorst DC, Jager KJ, van Dijk PC, Tomas LM, Ansell D, Collart F, Finne P, Heaf JG, De Meester J, Wetzels JF, Rosendaal FR, Dekker FW: Cardiovascular and noncardiovascular mortality among patients starting dialysis. JAMA 2009, 302: 1782–1789
5. Sarnak MJ, Levey AS, Schoolwerth AC, Coresh J, Culleton B, Hamm LL, McCullough PA, Kasiske BL, Kelepouris E, Klag MJ, Parfrey P, Pfeffer M, Raij L, Spinosa DJ, Wilson PW: Kidney disease as a risk factor for development of cardiovascular disease: a statement from the American Heart Association councils on kidney in cardiovascular disease, high blood pressure research, clinical cardiology, and epidemiology and prevention. Hypertension 2003, 42:1050–1065
6. Fellstrom BC, Jardine AG, Schmieder RE, Holdaas H, Bannister K, Beutler J, Chae DW, Chevaile A, Cobbe SM, Gronhagen-Riska C, De Lima JJ, Lins R, Mayer G, McMahon AW, Parving HH, Remuzzi G, Samuelsson O, Sonkodi S, Sci D, Suleymanlar G, Tsakiris D, Tesar V, Todorov V, Wiecek A, Wuthrich RP, Gottlow M, Johnsson E, Zannad F: Rosuvastatin and cardiovascular events in patients undergoing hemodialysis. N Engl J Med 2009, 360:1395–1407
7. Baigent C, Landray MJ, Reith C, Emberson J, Wheeler DC, Tomson C, et al: The effects of lowering LDL cholesterol with simvastatin plus ezetimibe in patients with chronic kidney disease (study of heart and renal protection): a randomised placebo-controlled trial. Lancet 2011, 377:2181–2192
8. Hansson GK: Inflammation, atherosclerosis, and coronary artery disease. N Engl J Med 2005, 352:1685–1695
9. Libby P, Aikawa M: Stabilization of atherosclerotic plaques: new mechanisms and clinical targets. Nat Med 2002, 8:1257–1262
10. Businaro R, Tagliani A, Buttari B, Profumo E, Ippoliti F, Di Cristofano C, Capoano R, Salvati B, Rigano R: Cellular and molecular players in the atherosclerotic plaque progression. Ann N Y Acad Sci 2012, 1262:134–141
11. McIntyre CW, Harrison LE, Eldehni MT, Jefferies HJ, Szeto CC, John SG, Sigrist MK, Burton JO, Hothi D, Korsheed S, Owen PJ, Lai KB, Li PK: Circulating endotoxemia: a novel factor in systemic inflammation and cardiovascular disease in chronic kidney disease. Clin J Am Soc Nephrol 2011, 6:133–141
12. Navarro-Gonzalez JF, Mora-Fernandez C, Muros M, Herrera H, Garcia J: Mineral metabolism and inflammation in chronic kidney disease patients: a cross-sectional study. Clin J Am Soc Nephrol 2009, 4:1646–1654
13. Chen HY, Chiu YL, Hsu SP, Pai MF, Lai CF, Yang JY, Peng YS, Tsai TJ, Wu KD: Elevated C-reactive protein level in hemodialysis patients with moderate/severe uremic pruritus: a potential mediator of high overall mortality. QJM 2010, 103:837–846
14. Lam MF, Leung JC, Lam CW, Tse KC, Lo WK, Lui SL, Chan TM, Tam S, Lai KN: Procalcitonin fails to differentiate inflammatory status or predict long-term outcomes in peritoneal dialysis-associated peritonitis. Perit Dial Int 2008, 28:377–384

15. Pan L, Li Y, Jia L, Qin Y, Qi G, Cheng J, Qi Y, Li H, Du J: Cathepsin S deficiency results in abnormal accumulation of autophagosomes in macrophages and enhances Ang II-induced cardiac inflammation. PLoS One 2012, 7:e35315
16. Lohoefer F, Reeps C, Lipp C, Rudelius M, Zimmermann A, Ockert S, Eckstein HH, Pelisek J: Histopathological analysis of cellular localization of cathepsins in abdominal aortic aneurysm wall. Int J Exp Pathol 2012, 93:252−258
17. Samouillan V, Dandurand J, Nasarre L, Badimon L, Lacabanne C, Llorente-Cortes V: Lipid loading of human vascular smooth muscle cells induces changes in tropoelastin protein levels and physical structure. Biophys J 2012, 103:532−540
18. Simpson CL, Lindley S, Eisenberg C, Basalyga DM, Starcher BC, Simionescu DT, Vyavahare NR: Toward cell therapy for vascular calcification: osteoclast-mediated demineralization of calcified elastin. Cardiovasc Pathol 2007, 16:29−37
19. Liu J, Sukhova GK, Sun JS, Xu WH, Libby P, Shi GP: Lysosomal cysteine proteases in atherosclerosis. Arterioscler Thromb Vasc Biol 2004, 24:1359−1366
20. Samokhin AO, Lythgo PA, Gauthier JY, Percival MD, Bromme D: Pharmacological inhibition of cathepsin S decreases atherosclerotic lesions in apoe-/- mice. J Cardiovasc Pharmacol 2010, 56:98−105
21. Aikawa E, Aikawa M, Libby P, Figueiredo JL, Rusanescu G, Iwamoto Y, Fukuda D, Kohler RH, Shi GP, Jaffer FA, Weissleder R: Arterial and aortic valve calcification abolished by elastolytic cathepsin S deficiency in chronic renal disease. Circulation 2009, 119:1785−1794
22. Bro S, Bentzon JF, Falk E, Andersen CB, Olgaard K, Nielsen LB: Chronic renal failure accelerates atherogenesis in apolipoprotein E-deficient mice. J Am Soc Nephrol 2003, 14:2466−2474
23. Aikawa E, Nahrendorf M, Figueiredo JL, Swirski FK, Shtatland T, Kohler RH, Jaffer FA, Aikawa M, Weissleder R: Osteogenesis associates with inflammation in early-stage atherosclerosis evaluated by molecular imaging in vivo. Circulation 2007, 116:2841−2850
24. Aikawa E, Nahrendorf M, Sosnovik D, Lok VM, Jaffer FA, Aikawa M, Weissleder R: Multimodality molecular imaging identifies proteolytic and osteogenic activities in early aortic valve disease. Circulation 2007, 115:377−386
25. Qin Y, Cao X, Guo J, Zhang Y, Pan L, Zhang H, Li H, Tang C, Du J, Shi GP: Deficiency of cathepsin S attenuates angiotensin II-induced abdominal aortic aneurysm formation in apolipoprotein E-deficient mice. Cardiovasc Res 2012, 96:401−410
26. Sukhova GK, Zhang Y, Pan JH, Wada Y, Yamamoto T, Naito M, Kodama T, Tsimikas S, Witztum JL, Lu ML, Sakara Y, Chin MT, Libby P, Shi GP: Deficiency of cathepsin S reduces atherosclerosis in LDL receptor-deficient mice. J Clin Invest 2003, 111:897−906
27. Aikawa M, Libby P: The vulnerable atherosclerotic plaque: pathogenesis and therapeutic approach. Cardiovasc Pathol 2004, 13: 125−138
28. Zhang M, Lu S, Wu X, Chen Y, Song X, Jin Z, Li H, Zhou Y, Chen F, Huo Y: Multimarker approach for the prediction of cardiovascular events in patients with mild to moderate coronary artery lesions. a 3-year follow-up study. Int Heart J 2012, 53:85−90
29. Breit SN, Carrero JJ, Tsai VW, Yagoutifam N, Luo W, Kuffner T, Bauskin AR, Wu L, Jiang L, Barany P, Heimburger O, Murikami MA, Apple FS, Marquis CP, Macia L, Lin S, Sainsbury A, Herzog H, Law M, Stenvinkel P, Brown DA: Macrophage inhibitory cytokine-1 (mic-1/gdf15) and mortality in end-stage renal disease. Nephrol Dial Transplant 2012, 27:70−75
30. Bootcov MR, Bauskin AR, Valenzuela SM, Moore AG, Bansal M, He XY, Zhang HP, Donnellan M, Mahler S, Pryor K, Walsh BJ, Nicholson RC, Fairlie WD, Por SB, Robbins JM, Breit SN: Mic-1, a novel macrophage inhibitory cytokine, is a divergent member of the TGF-beta superfamily. Proc Natl Acad Sci U S A 1997, 94: 11514−11519
31. de Jager SC, Bermudez B, Bot I, Koenen RR, Bot M, Kavelaars A, de Waard V, Heijnen CJ, Muriana FJ, Weber C, van Berkel TJ, Kuiper J, Lee SJ, Abia R, Biessen EA: Growth differentiation factor 15 deficiency protects against atherosclerosis by attenuating CCR2-mediated macrophage chemotaxis. J Exp Med 2011, 208:217−225
32. Bania J, Gatti E, Lelouard H, David A, Cappello F, Weber E, Camosseto V, Pierre P: Human cathepsin S, but not cathepsin l, degrades efficiently MHC class II-associated invariant chain in nonprofessional APCs. Proc Natl Acad Sci U S A 2003, 100: 6664−6669
33. Beers C, Burich A, Kleijmeer MJ, Griffith JM, Wong P, Rudensky AY: Cathepsin S controls MHC class II-mediated antigen presentation by epithelial cells in vivo. J Immunol 2005, 174: 1205−1212